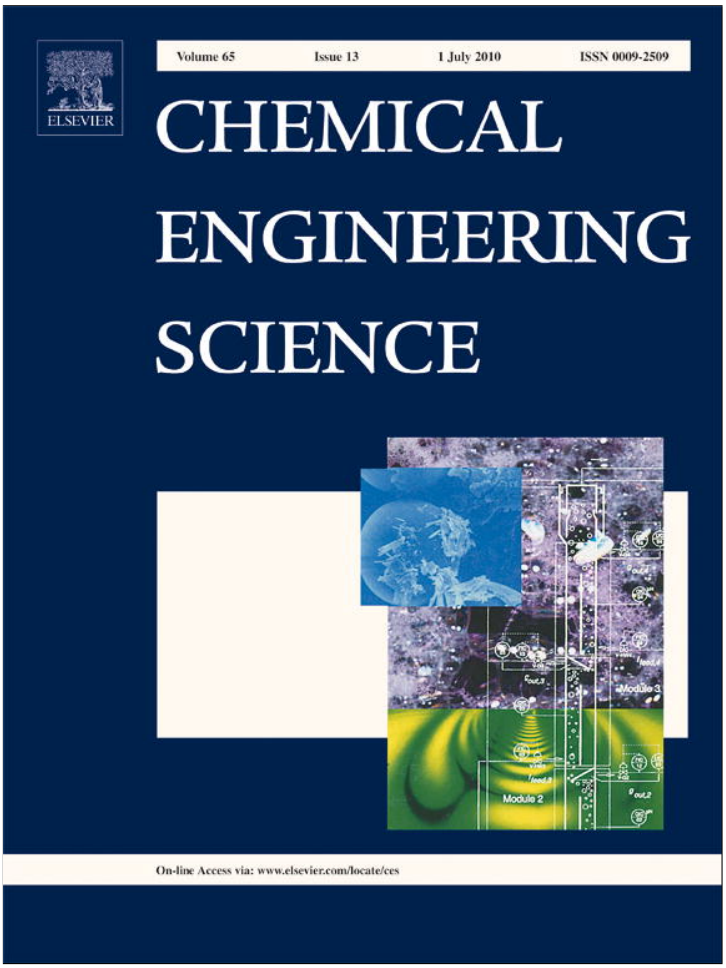

Chemical Engineering Science 65 (2010) 3947–3956

Contents lists available at ScienceDirect

Chemical Engineering Science

journal homepage: www.elsevier.com/locate/ces

Liquid–liquid two-phase flow and mass transfer characteristics in packed microchannels

Yuanhai Su [a,b], Yuchao Zhao [a], Guangwen Chen [a,*], Quan Yuan [a]

[a] Dalian National Laboratory for Clean Energy, Dalian Institute of Chemical Physics, Chinese Academy of Sciences, Dalian 116023, China
[b] Graduate University, Chinese Academy of Sciences, Beijing 100049, China

ARTICLE INFO

Article history:
Received 7 October 2009
Received in revised form
3 March 2010
Accepted 22 March 2010
Available online 2 April 2010

Keywords:
Microchannel
Extraction
Mixing
Immiscible fluids
Mass transfer
Multiphase flow

ABSTRACT

In this work, the flow hydrodynamic characteristics and the mass transfer performance of immiscible fluids in the packed microchannels are investigated experimentally. Water–kerosene system is used for visually identifying the flow hydrodynamic characteristics in PMMA microchannels, and water–succinic acid–n-butanol is chosen for investigating mass transfer performance in stainless steel microchannels. Quartz sand micro-particles are used as packing particles. In packed microchannels, high liquid–liquid dispersions can be obtained, and the diameter of droplets produced in the packed microchannel can be even less than 10 μm. It ensures better mixing performance and larger effective interfacial area of two immiscible fluids, and improves the mass transfer performance obviously. Compared to the extraction efficiency (46–61%) in the non-packed microchannel, it can reach 81–96% in the packed microchannel. The effects of packing length, micro-particle size on liquid–liquid dispersions and extraction efficiency are investigated. The pressure drop and the specific energy dissipation in the packed microchannels are also discussed.

1. Introduction

Liquid–liquid extraction is widely used in process industry, such as petroleum, food, hydrometallurgy, and chemical industries (Laddha and Degaleesan, 1978). Although many extractors including settler cascade, sieve plate, pulsed, and rotating disc extraction columns have been developed, few meet the high performance needs for many new separation processes and the development of more efficient equipments is needed. Generally, the size of the droplets produced by these traditional extractors is in the range of 0.1–3 mm (Rowe et al., 1965). Therefore, the effective interfacial area is not enough, and diffusion distance is too long. The mass transfer is an important step in extraction process; in other words, an improved mass transfer condition may benefit the whole extraction process. In addition, many fast or instantaneous liquid–liquid heterogeneous reactions are also limited by mass transfer; thus, the mixing and the mass transfer of immiscible liquid–liquid two phases between them are very important.

One major area in chemical engineering is process intensification (Burns et al., 2000; Gerven and Stankiewicz, 2009; Harmsen, 2007; Kochmann, 2007), which benefits from the miniaturization of channels and ducts within devices, where the characteristic lengths reach the scale of boundary layers thickness. Microchemical engineering technology as a novel process intensification method of chemical process has attracted many researchers from the 1990s (Ge et al., 2005; Hessel and Löwe, 2003; Jähnisch et al., 2004; Odedra et al., 2008; Wiles and Watts, 2008). Due to the extremely large surface-to-volume ratio and the short transport path in microreactors, its unique features, such as fast mixing and heat transfer, can be used for the controlling of extreme reactions in chemical industry. Now the liquid–liquid two-phase reactions in microreactor are mostly focused on nitration (Burns and Ramshaw, 2002), diazo-reaction (SalimiMoosavi et al., 1997), nanoparticles synthesis (Ying et al., 2008), etc. Benz et al. (2001) reported the microstructured equipments used for extraction process. The flow hydrodynamic and mass transfer characteristics of immiscible fluids in T-shaped microchannels have also been investigated in our group (Yue et al., 2007; Zhao et al., 2006, 2007). Other research about extraction in microchannels were also reported (Aota et al., 2007; Maruyama et al., 2004a, 2004b; Tokeshi et al., 2002), but most of them were mainly emphasized in analytical chemistry, their throughput was very low and the operating conditions were rigorous.

Generally, the flow in microreactors is laminar, and the mixing is mainly driven by molecular diffusion. To reduce the diffusion distance and thus to shorten the mixing time, reactant fluids are split into many laminated fluids in several micromixers, such as interdigital micromixer (Ehrfeld et al., 1999), static V-micro-jet mixer (Ehlers et al., 2000), static micromixer (Bertsch et al., 2001).

* Corresponding author. Tel.: +86 411 8437 9031; fax: +86 411 8469 1570.
E-mail address: gwchen@dicp.ac.cn (G. Chen).

0009-2509/$ - see front matter © 2010 Elsevier Ltd. All rights reserved.
doi:10.1016/j.ces.2010.03.034

Furthermore, the micromixers have experienced quick development, and other different types have occurred in recent years. Nagasawa et al. (2005) had designed a new type of micromixer for rapid mixing by both kinetic energy and molecular diffusion of fluids. The rapid mixing was realized by the collision of microsegments, which were divided into several radial streams at the center of the mixer. Good mixing performance came true by flow splitting, recombination, and rearrangement in split-and-recombine micromixer (Schönfeld et al., 2004). Kim et al. (2009) proposed a multifunctional micromixer based on an array of planar asymmetric microelectrodes with a diagonal or herringbone shape that produced alternating current electroosmotic flow. Their results showed the enhancement of mixing was carried out through the herringbone electrode configuration compared with a reference. However, these micromixers are difficult to manufacture due to the complexity of their structure. In addition, the main disadvantage of these mixers is that an initially finely generated dispersion soon experiences coalescence. T-shaped microchannel is easy to design and manufacture, so it is widely used in laboratory. Nevertheless, T-shaped microchannel is difficult to provide micro-droplets smaller than 100 μm according to existing reports; thus it cannot get high extraction efficiency when it is used as a kind of extractor.

Currently, droplets flow of immiscible liquid–liquid two phases as dispersed phase flow pattern in microchannels has been paid attention by many researchers due to the internal circulation within droplets (Bringer et al., 2004; Burns and Ramshaw, 2001; Matsuyama et al., 2007). Tice et al. (2003) investigated the rapid mixing of multiple reagents isolated in droplets, and they considered that winding microchannels make chaotic advection appear in droplets by internal circulation, which can stretch and fold the fluids striation, eventually the intensification of mixing in droplets can be obtained. Matsuyama et al. (2007) demonstrated experimentally that the two miscible liquids slug droplets could be formed by introducing the immiscible carrier phase, and showed this slug-based microfluidics could offer rapid mixing and the reactant arrangements by internal circulation in slug. Reactions in droplets in microfluidic channels have also attracted many researchers due to the elimination of Taylor dispersion by internal circulation, such as the measurement of fast reaction kinetics parameters (Song et al., 2003), protein crystallization (Zheng et al., 2004) synthesis of nanoparticles (Khan and Jensen, 2007), etc. However, only under very low flow velocity or extremely large volumetric flux ratio of immiscible liquid–liquid two phases, the droplets flow can be obtained in microchannels. Therefore, we consider a suitable method to produce dispersed phase flow pattern in microchannels.

As previously mentioned, if the overall mass transfer coefficient or the effective interfacial area is improved, the mass transfer in extraction process may be intensified. The hydrodynamics and contact of the immiscible liquid–liquid two phases must be improved for achieving better mass transfer performance. According to existing models of liquid–liquid two-phase mass transfer (Kronig and Brink, 1950), the droplet size is one of the main factors that influence the overall mass transfer coefficient and the effective interfacial area. In order to investigate the effects of the droplet size on the effective interfacial area, we make a simplified assumption that if a larger droplet (1 mm) is divided into some smaller droplets (10 μm), the interfacial area will increase about 100 times.

In a previous work (Su et al., 2009), we found a new method that intensified the liquid–liquid two-phase mass transfer process dramatically by gas agitation in microchannels. Now, we propose another new method that can further intensify mass transfer process between the immiscible liquid–liquid two phases in T-shaped microchannels by packing micro-particles. The effects of micro-particles on the flow characteristics and mass transfer of the two immiscible fluids are investigated in PMMA substrate microchannels and stainless steel microchannels, respectively.

2. Experimental section

2.1. Material and apparatus

The essential features of the packed microchannel are shown in Fig. 1. Quartz sand micro-particles are packed in the microchannel of one plate sparsely. The packing length of micro-particles is proportional to the weight of micro-particles for regularity and reproduction, and the porosity is 0.61. In order to prevent the loss of micro-particles, a bundle of glass fiber whose length is about 2 mm is placed in the rear of the packing section. And then another plate is used as cover plate, and the two plates are compressed each by bolts. Two opposing streams enter coaxially from the two inlet arms, begin to contact in T-junction, and flow along the main channel packed with micro-particles, and then leave from the outlet. To accurately investigate the mass transfer process in the whole packed microchannel, the main channel is divided into three mass transfer zones, that is, mass transfer zone-1 (from T-junction to packed micro-particles), mass transfer zone-2 (the packing section) and mass transfer zone-3 (from the downstream of packed micro-particles to the outlet of microchannel). Here, the length of mass transfer zone-2 can be changed by changing the packing length.

Water–kerosene is used for visually identifying flow characteristics of two immiscible fluids, and water–succinic acid–*n*-butanol is chosen for investigating mass transfer performance. The de-ionized water is used in all the experiments. Succinic acid and *n*-butanol are of analytical grade. The physical properties of the working systems are listed in Table 1. Minute amounts of methylene blue are dissolved in water for better visualization of the flow phenomena in flow experiment. The organic (*n*-butanol) and aqueous phases (water) are always mutually saturated to prevent multicomponent diffusion in the two phases; therefore, succinic acid as the only diffusing species transferred from organic phase to aqueous phase. Two kinds of average size quartz sand micro-particles are used as packing particles, their

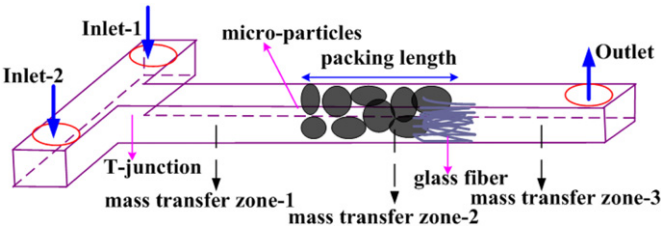

Fig. 1. Schematic of the packed microchannel.

Table 1
The properties of the working systems (at 293 K and atmospheric pressure).

Working systems	Density (kg/m^3)	Viscosity (mPa s)
Saturated deionized water with *n*-butanol	981.7	1.05
Saturated *n*-butanol with deionized water	837	3.34
Kerosene	780	1.15
Succinic acid	1552	–

average diameters (d) are 250 μm (Type-1) and 350 μm (Type-2), respectively.

The typical T-shaped microchannels are fabricated in two kinds of materials by micromachining technology. The depth, width, and length of two kinds of microchannels are 600 μm, 600 μm, and 60 mm, respectively. The transparent PMMA substrate microchannel is used for visually identifying flow characteristics of two immiscible fluids, in which flow pattern could be observed with high-speed CCD camera that is connected to a personal computer and provided snapshots. The average diameters of droplets are obtained by measuring 25 droplets in the same recorded photograph using image-analysis software. Due to the swelling of n-butanol on PMMA material, the measurement of mass transfer performance was carried out in the stainless steel microchannel. Table 2 shows the dimensions of two kinds of rectangular microchannels.

2.2. Experimental setup

The schematic diagram of the experimental apparatus is shown in Fig. 2. To maintain continuous flow without pulsation, two high precision piston pumps (Beijing Satellite Manufacturing Factory) and two check valves are used. The aqueous and organic phases are forced to flow through the horizontal rectangular microchannel by these high precision piston pumps, respectively.

In all experimental runs, the volume flux ratio of organic phase to aqueous phase (q) is adjusted to 1; the inlet pressure is measured with a pressure transducer. Separatory funnel is directly used to collect samples from the outlet streams, and the two immiscible phases could be separated immediately after sampling. The sampling time is short in order to avoid mass transfer during sample collection process as much as possible. The succinic acid concentrations of the two phases at the inlet and outlet of the T-shaped microchannel are measured via titration. Each experimental run is repeated at least two times, and each data point represents the mean value of at least two measurements of the outlet concentration of organic phase and aqueous phase, and the relative deviation does not exceed $\pm 5\%$ in all the experiments.

Table 2
Dimensions of T-shaped microchannel.

Inlet-1 and inlet-2 arms			Mixing channel		
W (μm)	H (μm)	L_0 (mm)	W (μm)	H (μm)	L_0 (mm)
600	600	15	600	600	60

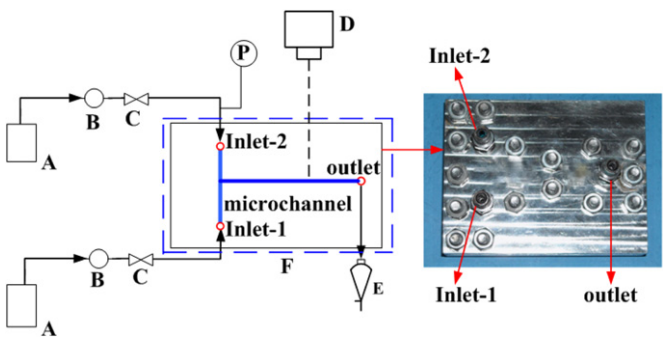

Fig. 2. Schematic diagram of experimental setup: (A) liquid tank, (B) piston pump, (C) check valve, (D) CCD, (E) separatory funnel, and (F) microchannel.

3. Results and discussion

3.1. Definitions of relevant parameters

The extraction efficiency can be expressed as follows:

$$E = \frac{C_{aq,i} - C_{aq,o}}{C_{aq,i} - C^*_{aq,o}} \tag{1}$$

where $C_{aq,j}$ and $C_{aq,o}$ are concentrations of the solute in the inlet aqueous phase and in the aqueous phase after phases separating, respectively. $C^*_{aq,o}$ is equilibrium concentration of the solutes in the outlet aqueous phase corresponding to the actual outlet concentration of the solutes in the organic phase, respectively. The Reynolds numbers of the two immiscible phases are defined similar to a previous work (Su et al., 2009):

$$Re_M = \frac{D_e U_M \rho_M}{\mu_M} \tag{2}$$

$$U_M = \frac{Q_{aq} + Q_{or}}{A} \tag{3}$$

$$D_e = \frac{4A}{2(W+H)} \tag{4}$$

$$\rho_M = \left(\frac{\theta_{aq}}{\rho_{aq}} + \frac{1-\theta_{aq}}{\rho_{or}}\right)^{-1} \tag{5}$$

$$\mu_M = \left(\frac{\theta_{aq}}{\mu_{aq}} + \frac{1-\theta_{aq}}{\mu_{or}}\right)^{-1} \tag{6}$$

where D_e, Q_{aq}, Q_{or}, U_M, ρ_M, and μ_M are the hydraulic diameter of microchannel, volumetric flow rate of aqueous, volumetric flow rate of organic solutions, the total superficial flow rate of the immiscible liquid–liquid two phases, the mixture viscosity, and the mixture density, respectively.

Because the effective interfacial area between the immiscible phases in the extraction is not known, the overall volumetric mass transfer coefficients (ka) are determined from the experimental results. The ka is normally defined by the following:

$$R = Q_{or}(C_{or,i} - C_{or,o}) = kaV\Delta C_m \tag{7}$$

$$ka = \frac{Q_{or}(C_{or,i} - C_{or,o})}{V\Delta C_m} \tag{8}$$

$$\Delta C_m = \frac{(C_{or,i} - C^*_{or,i}) - (C_{or,o} - C^*_{or,o})}{\ln\left[\frac{(C_{or,i} - C^*_{or,i})}{(C_{or,o} - C^*_{or,o})}\right]} \tag{9}$$

where a, V, R, and ΔC_m are the interfacial mass transfer area between the phases per unit volume of the microchannel, microchannel volume, extraction rates, and logarithmic mean concentration driving force, respectively. $C^*_{or,i}$ is the equilibrium concentration of the solutes in the inlet organic phase, corresponding to the actual inlet concentration of the solutes in the aqueous phase, and $C^*_{or,o}$ is the equilibrium concentration of the solutes in the outlet organic phase, corresponding to the actual outlet concentration of the solutes in the aqueous phase.

3.2. Effects of micro-particles on the dispersion

Although much attention has been given to the slug flow due to its special characteristics, parallel flow (continuous phase flow pattern) exists over a wide range of phase flow rates according to the flow patterns of immiscible liquid–liquid two-phase in the microchannel (Zhao et al., 2006). During all fluid flow

experimental runs in this paper, the water phase and the kerosene phase form parallel flow in non-packed microchannel as shown in Fig. 3. The interface of the two phases can be smooth or wavy at the T-junction depending on the flow rate of the immiscible two phases. However, it eventually evolves into a smooth interface in the fully developed flow due to the viscous friction force.

In the microscale system, the interface effect is more obvious compared to the conventional scale. In the packed microchannel, the quartz sand micro-particles are hydrophilic and provide more contact area compared with the microchannel wall. Therefore, the organic phase is prone to form a dispersed phase. From the experimental observations, the kerosene phase forms dispersed droplets in the packed PMMA substrate microchannel. So it can be deduced that *n*-butanol phase will form dispersed droplets in the packed stainless steel microchannel even though we cannot observe the flow phenomena. Fig. 4 shows the effects of the flow rate on the dispersion of organic phase in a packed microhannel. The liquid–liquid dispersion photographs corresponding to the different flow rates are placed in the figure, and the average diameter of droplets is obtained through them. Type-1 micro-particles are packed in the middle section of the microchannel and the packing length (L) is 6.5 mm, the observation point locates downstream of the packed particles and adjoins them. As shown in Fig. 4, it is clear that an increase of flow rate leads to smaller droplets. The average diameter of droplets decreases from 106 to 15 μm, and the corresponding effective interracial area is in the range of 14,150–100,000 m^2/m^3, when aqueous phase superficial velocity increases from 0.023 to 0.185 m/s. The average diameter of droplets is much less than microchannel characteristic length. As aqueous phase velocity is up to 0.255 m/s, the droplet size is even less than the minimum detection value of the high-speed CCD camera (the minimum measurable droplet diameter is about 10 μm for this shooting system). Under this operational condition, the two immiscible fluids mix acutely, their interface is difficult to distinguish and effective interfacial area is very large.

Fig. 5 shows the effects of packing length of micro-particles on the dispersion of organic phases in packed-bed microhannels.

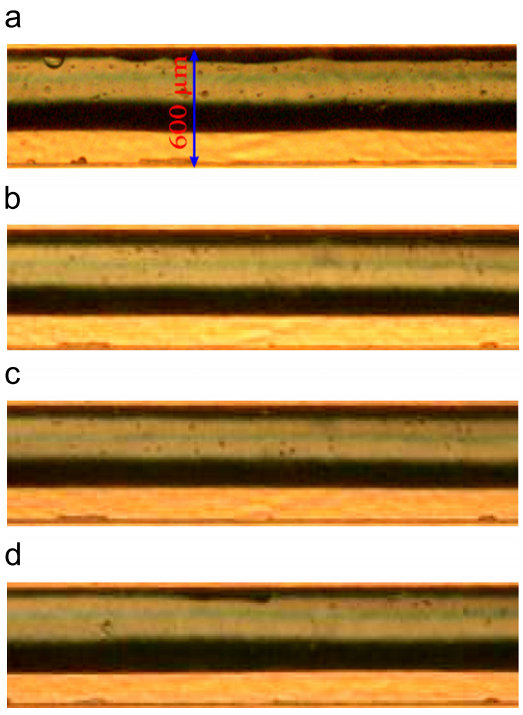

Fig. 3. Parallel flow patterns of liquid–liquid two phases in the non-packed microchannel $U_{or}=U_{aq}$ (m/s): (a) 0.046, (b) 0.139, (c) 0.255, and (d) 0.463.

Type-1 micro-particles are packed in the front of the microchannel with the distance about 10 mm between them and T-junction. It can be seen that the dispersion performance of 6.5 mm packing length is better than that of 3.5 mm packing length. The average diameter of droplets produced in microchannel with 6.5 mm packing length is approximately half of that produced in microchannel with 3.5 mm packing length, as the aqueous phase velocity increases from 0.046 to 0.185 m/s. The minimum average diameter of droplets produced in microchannel with 6.5 mm packing length even reaches 13 μm when the aqueous phase velocity is 0.185 m/s. Based on the above discussion, we can know the longer packing length leads to the better dispersion performance. From Figs. 4 and 5, we can also see the packing position may have effects on the liquid–liquid dispersion. Under the same packing length (L=6.5 mm) and the same flow rate, packing in the front of microchannel leads to smaller droplets compared with packing in the middle section of

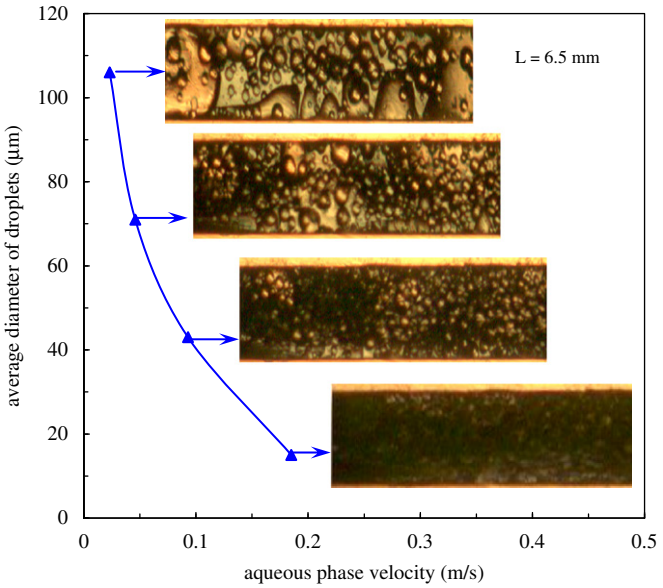

Fig. 4. Effects of flow rate on the average diameter of droplets in packed-bed microhannel.

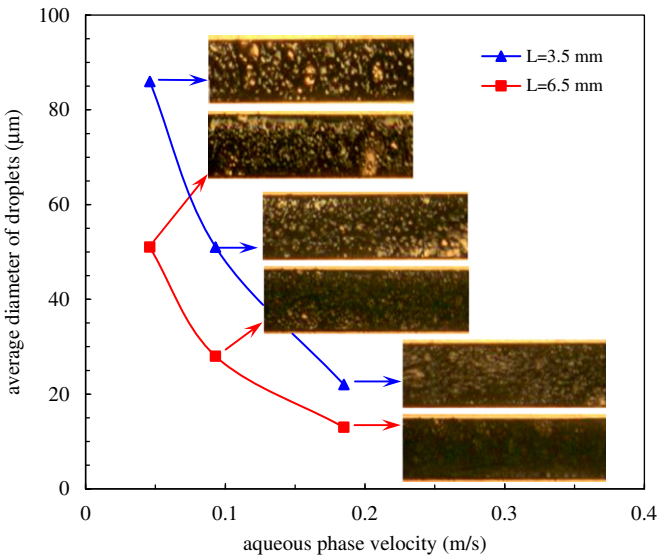

Fig. 5. Effects of packing length on the dispersion in the packed microchannel.

the microchannel. Based on our previous work (Zhao et al., 2007), the interface disturbance of the immiscible liquid–liquid two phases is most drastic in the T-junction of the microchannel. In the packed microchannel, the effect of T-junction also cannot be neglected. Therefore, if the packing position is closer to T-junction, better dispersion performance will be obtained.

Losey et al. (2001) had studied characterization of mass transfer and reactions in microfabricated multiphase packed-bed reactors for gas–liquid reaction process. They found that the gas–liquid interface oscillated in a pulsing fashion, which could effectively improve the mass transfer performance. The flow characteristics of the immiscible liquid–liquid two phases in packed microchannels are complicated, and the interfacial effect is more significant compared with that of a conventional reactor. Fig. 6(a) and (b) shows the characteristics of the packed microchannel and the flow characteristics when two fluids flow through the interstices between micro-particles, respectively. As shown in Fig. 6(b), the two immiscible fluids flow into the confined and crooked interstices between micro-particles and mix acutely. In the extremely narrow micro-space, the two immiscible fluids interweave and shear each other. The irregular micro-particles that have higher surface area relative to that of the microchannel walls also shear the fluids drastically. Under the action of micro-particles, parallel flow transforms to the dispersed phase flow pattern and micro-droplets are formed easily. The shear effect of micro-particles increases with the increase of flow rate, thus leading to smaller droplets. The dispersion phenomena in the packed microchannel are not induced by the Rayleigh-Plateau instability, which leads to the formation of droplets in the microchannel (Link et al., 2004; Utada et al., 2005, 2008). Large interfacial area and high intensity interface disturbance of the immiscible liquid–liquid two phases are obtained in the packed microchannel.

3.3. *Effects of packing particles on mass transfer performance*

Effects of packing particles on mass transfer performance in microchannel are shown in Fig. 7. Type-2 micro-particles are packed in the rear of microchannel and their packing length is 12 mm. It appears that the overall volumetric mass transfer coefficients (ka) increase with increase in Re_M in the non-packed microchannel. Such a behavior is the consequence of increases in the surface renewal velocity and the effective interfacial area due to the interface disturbance of the two immiscible fluids. The values of ka also increase with increase in Re_M in the packed microchannel, which is similar to those of the non-packed microchannel. As discussed in the earlier section, when the micro-particles' packing length is fixed, an increase in flow rate

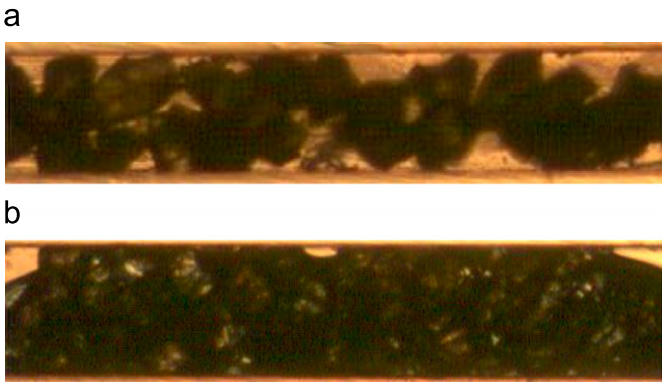

Fig. 6. The characteristics of packed microchannels without (a) and with (b) fluids flowing.

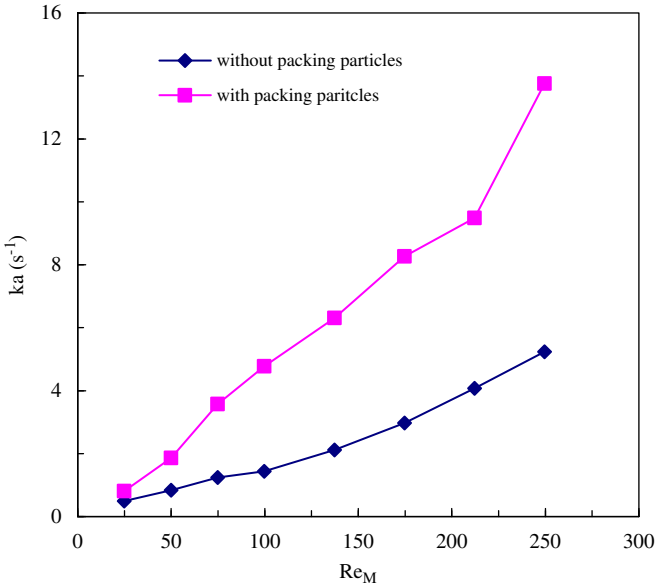

Fig. 7. Effects of micro-particles on the overall volumetric mass transfer coefficient.

leads to the formation of smaller droplets. As the flow rate increases to a certain degree, the average diameter of droplets produced is even less than the minimum detection value of the high-speed CCD camera; the interface of two immiscible fluids is difficult to distinguish and the interfacial mass transfer area is very large. The interface disturbance of the two immiscible fluids and the surface renewal velocity are enhanced with increase in Re_M; thus the overall volumetric mass transfer coefficients increase.

It is seen from Fig. 7 that the values of ka in the packed microchannel are two or three times higher than those in the non-packed microchannel. It is attributed to higher effective interfacial area and surface renewal velocity in the packed microchannel in comparison to the non-packed microchannel at the same flow rate. In mass transfer zone-1, the flow characteristic of two immiscible fluids and the mass transfer between them are recognized as the same as those in the non-packed microchannel. However, the characteristics of fluid flow and mass transfer in another two zones are different from those in the non-packed microchannel. In mass transfer zone-2, the immiscible fluids flow into the confined and crooked interstices between micro-particles and mix acutely. In the extremely narrow micro-space, the two immiscible fluids interweave and shear each other. The irregular micro-particles also shear the fluids drastically, which is beneficial to the mixing of two immiscible fluids. In comparison to parallel flow in non-packed microchannel, the effective interfacial area and surface renewal velocity in this zone can be enhanced; thus, the mass transfer performance is improved. In mass transfer zone-3, the mixture of two immiscible fluids flows from the downstream of packed micro-particles to the outlet of the microchannel. As discussed in the earlier section, in this zone of the packed microchannel, the dispersed phase flow pattern and the formation of micro-droplets can be obtained easily after the immiscible fluids flowing through the packing section. The organic phase droplets whose size is much smaller than the characteristic length of the microchannel collide with each other and the coalescence of droplets occurs in this zone of the packed microchannel. Actually, the dispersed droplets finally coalesce and form a continuous phase before sampling termination due to interface effect, which is needed for the separation of immiscible

liquid–liquid two phases. In addition, there is also internal circulation in droplets, which is beneficial to the increase of the surface renewal velocity (Bringer et al., 2004). The effective interfacial area and the surface renewal velocity are much larger than those in the non-packed microchannel. Therefore, the mass transfer process in this zone is also intensified.

Fig. 8 demonstrates the effects of packing particles on extraction efficiencies in microchannels. It is well known that extraction efficiency is the function of the overall volumetric mass transfer coefficients and residence time in mass transfer equipments. It can be expressed as the following equation: $E=f(ka, t)$. Generally, the value of ka increases with the increase in Reynolds number; contrarily, residence time decreases. In the non-packed microchannel, the extraction efficiency first decreases slightly with the increase in Re_M and then increases weakly. The maximum extraction efficiency does not exceed 61% in experimental runs. This is in accordance with the results of Benz et al. (2001). Based on the above discussion, we know an increase of Re_M will lead to the increase of the interface disturbance intensity and the surface renewal velocity; thus, the overall volumetric mass transfer coefficients also increase. Nevertheless, the residence time in microchannels decreases with the increase in Re_M. In the low flow rate region ($Re_M < 74.85$), the values of ka are low, and the residence time plays a dominant role, that is, the increase in residence time is the primary factor influencing extraction efficiency compared with the higher Re_M region. As Re_M increases, the residence time decreases, so the extraction efficiency decreases. As Re_M further increases, the increase of overall volumetric mass transfer coefficient plays a dominant role; in other words, the negative effect of the decrease in residence time is overcome, and accordingly, extraction efficiency increases slowly in the Re_M region ($74.85 < Re_M < 249.5$). In the packed microchannel, the extraction efficiency increases with the increase in Re_M in the low Re_M region ($Re_M < 74.85$), and then it mostly maintains at 93%. The maximum extraction efficiency is 96%, which almost achieves equilibrium stage. Large effective interfacial area and surface renewal velocity can be obtained in the packed microchannel even at low Re_M, so the overall volumetric mass transfer coefficient plays a dominant role relative to residence time. So extraction efficiency increases with the increase in Re_M, and then approaches the state of equilibrium stage.

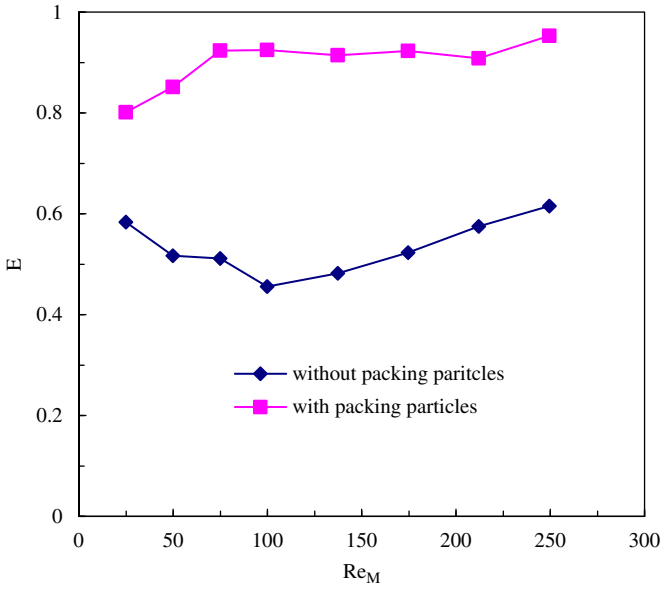

Fig. 8. Effects of packing micro-particles on extraction efficiency.

Even at low Re_M (Re_M=24.95), the extraction efficiency in packed microchannels can reach 80%, which is much higher than the maximum extraction efficiency in non-packed microchannels (61%). The residence time in the packed microchannel can be considered as the same as that in the non-packed microchannel at the same flow rate. However, the values of ka in the packed microchannel are two or three times higher than those in the non-packed microchannel. So extraction efficiencies are much higher than those in the non-packed microchannel.

3.4. Effects of packing length on extraction efficiency

The effects of the packing length of micro-particles on the extraction efficiency in the packed microchannel are shown in Fig. 9. Two kinds of average size micro-particles are used and packed in the rear of the microchannel. It can be seen that the extraction efficiency firstly increases obviously with the increase in relative packing length at different Re_M numbers, and then gradually tends to a fixed value. From the above discussion, we know that the dispersed droplet size is strongly dependent on the packing length. At the same Re_M number, an increase in packing length will lead to the formation of smaller droplets, that is, the dispersion performance becomes better. The mixing of two immiscible fluids and the effective interfacial area are improved with the increase in packing length; therefore, extraction efficiency increases. However, when the dispersed droplet size becomes small to a certain degree, it is hard to further break up the droplets, so the extraction efficiency increases weakly with the increase of the packing length.

3.5. Effects of micro-particle size on extraction efficiency

In order to investigate the effects of micro-particle size on extraction efficiency, two kinds of micro-particles whose average diameter are 250 and 350 μm are used, respectively. In this section, the packing length is 6.4 mm and the mass of micro-particles is 2.4 mg for these two kinds of micro-particles. As can be seen in Fig. 10, the extraction efficiency in the packed microchannel with Type-1 micro-particles is slightly better compared with those in the packed microchannel with Type-2 micro-particles when Re_M is identical. The result can be explained from the different dispersion performance of two kinds of micro-particles. The bulk density of micro-particles in the packed microchannel with Type-1 micro-particles is larger than that of the packed microchannel with Type-2 micro-particles, as shown in Fig. 11. And the packed microchannel with Type-1 micro-particles provides narrower micro-space, which is more beneficial to dispersion of organic phase into aqueous phase. For example, when the aqueous phase velocity is 0.023 m/s, the average diameters of droplets produced in the packed microchannel with Type-1 micro-particles and with Type-2 micro-particles are 150 μm (Fig. 12(a)) and 200 μm (Fig. 12(b)), respectively. As a consequence, higher effective interfacial area and extraction efficiency are obtained in the packed microchannel with smaller micro-particles.

3.6. Correlations of the mass transfer data

Predicting the mass transfer performance of packed microchannel is necessary for reactor optimization design. The Re_M and the packing length of micro-particles are the most important parameters based on the frontal discussions. The effect of Re_M can be expressed as Re_M^{α} in the correlations according to previous works (Su et al., 2009; Zhao et al., 2007). The mass transfer process between the immiscible liquid–liquid two phases can be

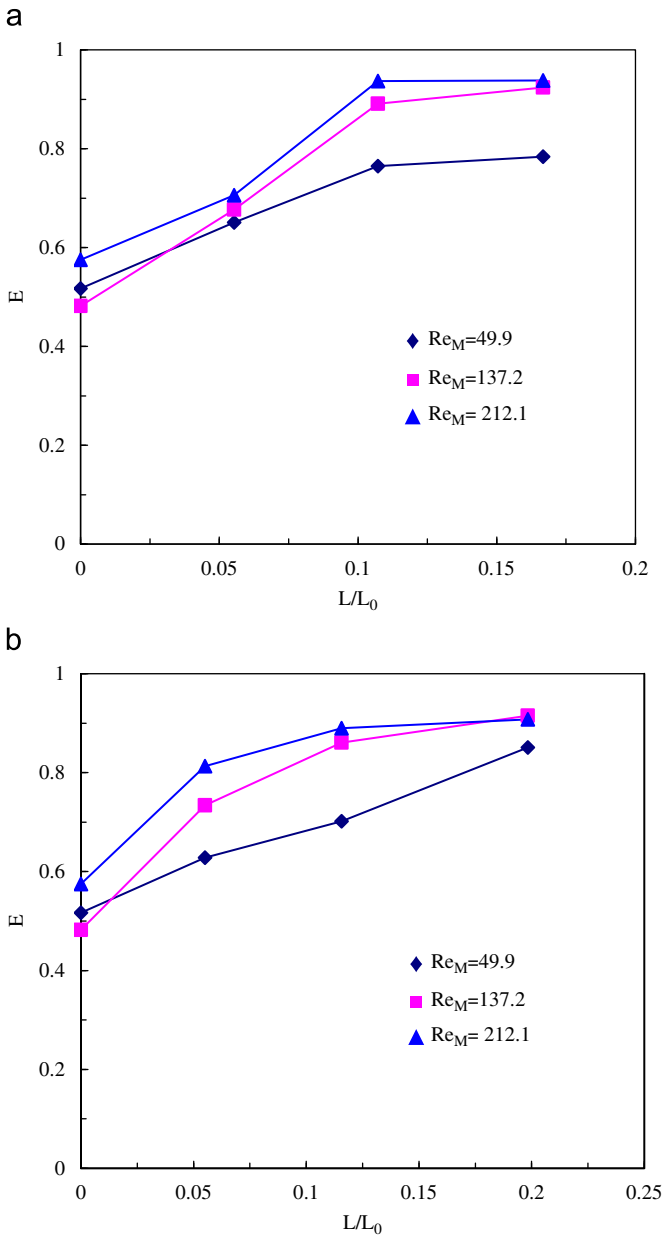

Fig. 9. Effects of the packing length on the extraction efficiency: (A) Type-1 micro-particles and (B) Type-2 micro-particles.

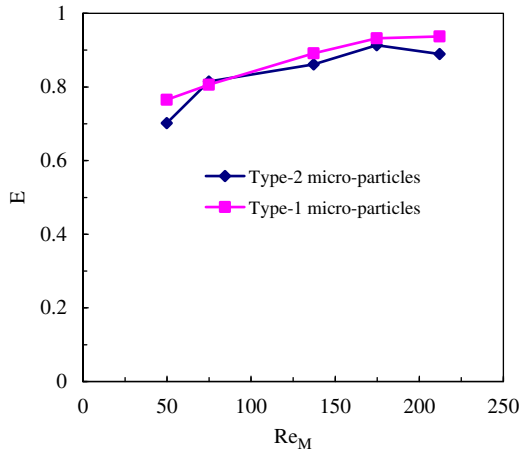

Fig. 10. Effects of micro-particles size on the extraction efficiency (L=6.4 mm).

intensified dramatically by micro-particles packing method. The factor $\exp(\beta(L/L_0))$ can be used to express the enhancement effect of micro-particles packing in the mass transfer process between the immiscible liquid–liquid two phases. As L/L_0 equals to zero, the factor $\exp(\beta(L/L_0))$ equals to 1, which represents the condition without micro-particles packing. The overall volumetric mass

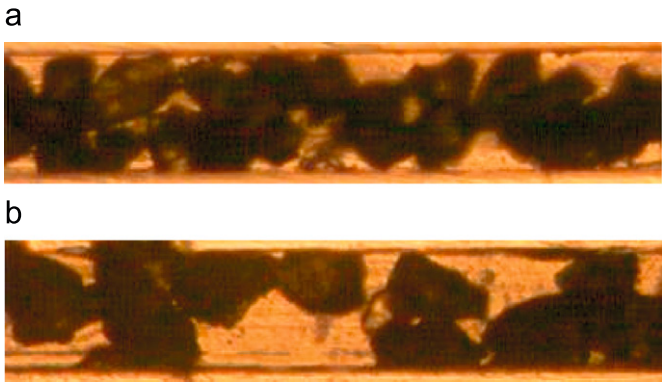

Fig. 11. The characteristics of packed microchannel with two kinds of micro-particles: (a) Type-1 micro-particles and (b) Type-2 micro-particles.

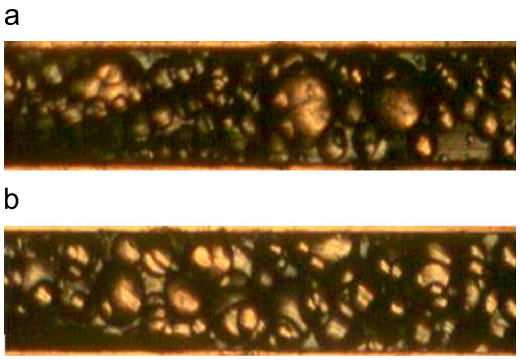

Fig. 12. Effects of micro-particle size on dispersion performance $U_{or}=U_{aq}$=0.023 m/s: (a) Type-1 micro-particles and (b) Type-2 micro-particles.

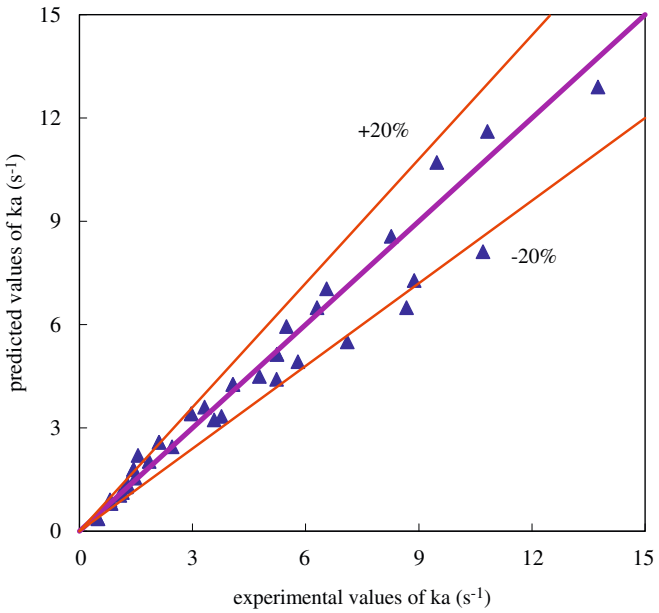

Fig. 13. Experimental vs. predicted values of *ka*.

transfer coefficients obtained from experimental data are correlated based on an analysis of multiple linear regression. It is found that the following correlations predict *ka* values well under the operation condition.

For the microchannel with packing Type-1 micro-particles

$$ka = 9 \times 10^{-3} Re_M^{1.15} \exp\left(6.01 \frac{L}{L_0}\right) \quad (10)$$

For the microchannel with packing Type-2 micro-particles

$$ka = 9 \times 10^{-3} Re_M^{1.15} \exp\left(4.64 \frac{L}{L_0}\right) \quad (11)$$

Fig. 13 demonstrates the experimental values of *ka* vs. the predicted values by Eqs. (10) and (11). The correlations predict the experimental data with relative deviation ±20%. From these correlations we can see the significant enhancement effects of packing micro-particles on mass transfer of immiscible liquid–liquid two phases in microchannels.

3.7. Pressure drop in packed microchannels

Fig. 14 shows the effects of the flow rate and the packing length on the pressure drop (ΔP) in packed microchannels with two kinds of micro-particles. The working system is water–*n*-butanol. The pressure drop increases with the increase in flow rate and packing length. The fluids only can flow through the confined interstices between micro-particles in packed microchannels. There is friction force between fluids and micro-particles, which increases with the increase in flow rate. The impinging of fluids on micro-particles and the sudden expansion or reduction of cross-section due to packing micro-particles also induce pressure drop, and their effects increase with the increase in flow rate and packing length. As a consequence, the pressure drop in packed microchannels is much higher than that in the non-packed microchannel.

In this section, the Ergun equation is used to predict pressure drop in packed microchannels. We make a simplified assumption that the packing condition keeps identical, and the immiscible liquid–liquid two phases are considered as homogeneous mixture base on a pseudo-homogeneous model. The Ergun equation is defined as follows:

$$\Delta P = \left[150 \frac{(1-\varepsilon)^2 U_M \mu_M}{\varepsilon^3 (\varphi_s d_e)^2} + 1.75 \frac{(1-\varepsilon)\rho_M U_M^2}{\varepsilon^3 (\varphi_s d_e)}\right] \times L \quad (12)$$

where ε is porosity, φ_s is average degree of sphericity of micro-particles, and d_e is equivalent diameter of packed microchannel. The relevant parameters of Ergun equation are listed in Table 3.

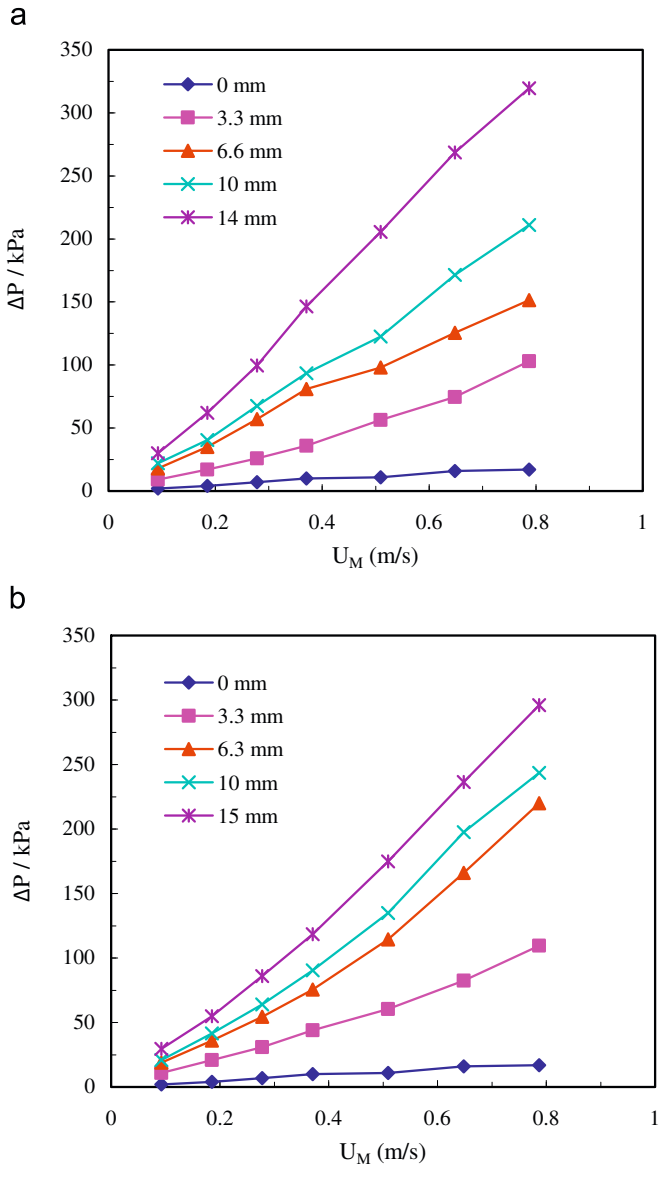

Fig. 14. Effects of U_M and L on ΔP in packed microchannels with two kinds of micro-particles: (A) Type-1 micro-particles and (B) Type-2 micro-particles.

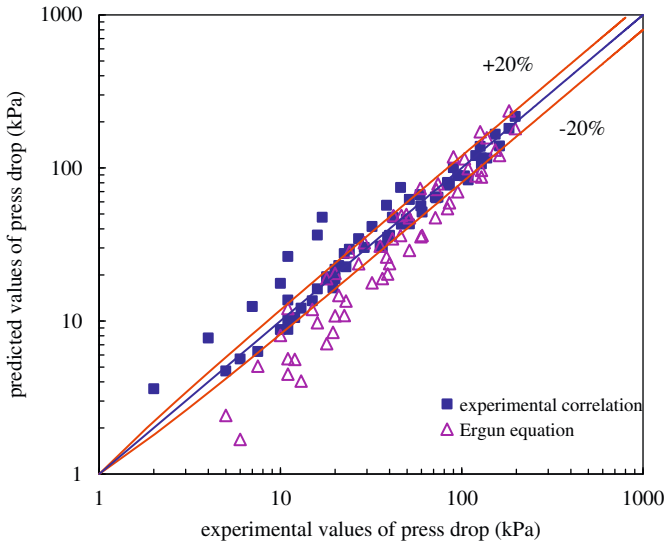

Fig. 15. The experimental values of ΔP vs. the predicted value.

Table 3
The relevant parameters of Ergun equation.

d_{e1} (10^{-6} m)	d_{e2} (10^{-6} m)	ρ_M (kg/m^3)	μ_M (Pa s)	δ (m^3/m^3)	φ_{s1} (m^2/m^2)	φ_{s2} (m^2/m^2)
208	255	903.6	0.002	0.61	0.8	0.7

Table 4
Comparison of mass transfer performance in different liquid–liquid contactors

Type	E (%)	$ka \times 10^4$ (s^{-1})	Volume (m^3)	Specific energy (W/kg) dissipation
Batch reactor (Cybulski et al., 2001)	–	0.16–16.6	1	10
Static mixer (Merchuk et al., 1980)	30–85	7.5–321	1.0×10^{-5}	180–3000
Packed microchannel (this work)	81–96	8000–1,30,000	1.0×10^{-8}	30–4900

Based on analysis of multiple linear regressions and the form of Ergun equation, a correlation is introduced, which further emphasizes the effect of micro-particles on pressure drop. The correlation is expressed as the following equation, where the total flow rate is in the range of 0.093–0.926 m/s:

$$\Delta P = (57.8U_M + 49.8U_M^2) exp\left(5.34\frac{L}{L_0}\right)\left(\frac{d}{D_e}\right)^{0.54} \quad (13)$$

It can be seen from Fig. 15 that most of the relative deviations between the experimental and predicted values of ΔP are in the range of -20–20% by Eq. (13). However, most of the predicted values of Ergun equation are less than the experimental values. It may be explained by the fact that the Ergun equation is not enough for the microscale system where interface effect is more obvious and needs to be considered. In addition, a part of pressure drop may result from a bundle of glass fiber, which is used for preventing micro-particles loss. It is hard to estimate this part of pressure drop. In order to decrease the pressure drop in packed microchannel, more appropriate packing method and more optimized micro-particles fixing method are required.

Merchuk et al. (1980) studied the efficiency of copper recovery from lean aqueous solutions with an organic solution of LIX-64N solvent in kerosene using static mixers. Their results showed that the higher efficiency was associated with the larger pressure drop. The mean specific energy dissipation (P_1) that describes the energy input into the microchannel system can be defined as follows:

$$P_1 = \frac{\Delta P Q}{G} \quad (14)$$

$$G = \rho_M V \quad (15)$$

where Q is the total volume flow rate and G is the mass into which the energy is dissipated. The characteristics of mass transfer and specific energy dissipation in different liquid–liquid contactors are listed in Table 4, where the relevant values are taken from pictures or tables presented in the literature (Cybulski et al., 2001; Kochmann, 2007; Merchuk et al., 1980). From Table 4, we can see that the values of ka obtained in the packed microchannel are more than three orders of magnitude higher than those in conventional batch reactor and static mixer, and the volume of microchannel is smaller by three or four orders of magnitude. The specific energy dissipation in the packed microchannel is at the same order of magnitude compared with static mixers, and about two orders of magnitude higher than that of batch reactor. Although the specific energy dissipation in the packed microchannel is higher than that in the batch reactor, better mass transfer performance and smaller system volume show its potential application. In addition, the packing micro-particles approach ensures larger effective interfacial area and better mixing of the immiscible liquid–liquid two phases; however, the characteristic dimensions of microchannels and the mass of packed particles must be well controlled and optimized to maintain an acceptable pressure drop for application.

4. Conclusions

A new method that intensifies the mass transfer of immiscible liquid–liquid two phases in the microchannel by packing micro-particles is investigated. It is found that high dispersion of aqueous phase and organic phase can be obtained in packed microchannel. The diameter of droplets produced in the packed microchannel is even less than 10 μm. The packing micro-particles approach ensures better mixing performance and larger effective interfacial area of two immiscible fluids, and improves the mass transfer performance obviously. The maximum extraction efficiency in the packed microchannel reaches 96%, which approaches equilibrium stage and is much higher than the maximum extraction efficiency in the non-packed microchannel (61%). Empirical correlations are developed based on the obtained data for estimating overall volumetric mass transfer coefficients and pressure drop of the immiscible liquid–liquid two phases in the packed microchannel. In addition, the characteristics of specific energy dissipation in different liquid–liquid contactors are discussed. Although the specific energy dissipation in the packed microchannel is larger, better mass transfer performance and smaller system volume show its potential application.

Notation

A	interfacial area, m^2/m^3
A	cross-sectional area of microchannel, m^2
C_{aq}	concentration of aqueous phase, mol/l
$C^*_{aq,o}$	equilibrium concentration of the solutes in the outlet aqueous phase corresponding to the actual outlet concentration of the solutes in the organic phase, mol/l
$C_{or,I}$	concentration of the solute in the inlet organic phase, mol/l
$C^*_{or,i}$	equilibrium concentration of the solutes in the inlet organic phase corresponding to the actual inlet concentration of the solutes in the aqueous phase, mol/l
$C_{or,o}$	concentration of the solute in the organic phase after phases separating, mol/l
$C^*_{or,o}$	equilibrium concentration of the solutes in the outlet organic phase corresponding to the actual outlet concentration of the solutes in the aqueous phase, mol/l
d	average diameter of micro-particles, m
d_e	equivalent diameter of packed microchannel, m
D_e	hydraulic diameter of microchannel, m
E	extraction efficiency, 1
H	microchannel height, m
k	overall mean mass transfer coefficient, m/s
ka	overall volumetric mean mass transfer coefficient,1/s
L	packing length of micro-particles, m
L_0	microchannel length, m
L/L_0	relative packing length of micro-particles
m	partition coefficient of solute between aqueous and organic phases

G	characteristic mass, kg
P_1	power consumed in mass transfer equipments, W/kg
ΔP	pressure drop, Pa
$q=Q_{or}/Q_{aq}$	volume flux ratio of organic phase to aqueous phase
Q	total volume flow rate, m^3/s
Q_{aq}	Aqueous phase volume flow rate, m^3/s
Q_{or}	organic phase volume flow rate, m^3/s
Re_M	Reynolds numbers of two immiscible phases, 1
T	superficial residence time in microchannel, s
U_{aq}	aqueous phase superficial velocity, m/s
U_M	total superficial velocity of the immiscible liquid–liquid two phases, m/s
U_{or}	organic phase superficial velocity, m/s
V	volume of microchannel, m^3
W	microchannel width, m

Greek letters

μ	viscosity, $Pa \cdot s$
ρ	mass density, kg/m^3
ε	porosity
θ	hold-up fraction
φ_s	average degree of sphericity of micro-particles

Subscripts

Aq	aqueous phase
i	inlet
M	mixture of the immiscible liquid–liquid two phases
o	outlet
or	organic phase
1	Type-1 micro-particles
2	Type-2 micro-particles

Acknowledgments

The work reported in this article was financially supported by research grants from the National Natural Science Foundation of China (Nos. 20911130358 and 20906087) and Ministry of Science and Technology of China (Nos. 2009CB219903 and 2007AA030206).

References

Aota, A., Nonaka, M., Hibara, A., Kitamori, T., 2007. Countercurrent laminar microflow for highly efficient solvent extraction. Angewandte Chemie International Edition 46, 878–880.

Benz, K., Jäckel, K.P., Regenauer, K.J., Schiewe, J., Drese, K., Ehrfeld, W., Hessel, V., Löwe, H., 2001. Utilization of micromixers for extraction processes. Chemical Engineering & Technology 24, 11–17.

Bertsch, A., Heimgartner, S., Cousseau, P., Renaud, P., 2001. Static micromixers based on large-scale industrial mixer geometry. Lab on a Chip 1, 56–60.

Bringer, M.R., Gerdts, C.J., Song, H., Tice, J.D., Ismagilov, R.F., 2004. Microfluidic systems for chemical kinetics that rely on chaotic mixing in droplets. Philosophical Transactions of the Royal Society of London Series A—Mathematical Physical and Engineering Sciences 362, 1087–1104.

Burns, J.R., Jamil, J.N., Ramshaw, C., 2000. Process intensification: operating characteristics of rotating packed beds—determination of liquid hold-up for a high-voidage structured packing. Chemical Engineering Science 55, 2401–2415.

Burns, J.R., Ramshaw, C., 2001. The intensification of rapid reactions in multiphase systems using slug flow in capillaries. Lab on a Chip 1, 10–15.

Burns, J.R., Ramshaw, C., 2002. A microreactor for the nitration of benzene and toluene. Chemical Engineering Communication 189, 1611–1628.

Cybulski, A., Moulijn, J.A., Sharma, M.M., Sheldon, Ra., 2001. Fine Chemicals Manufacture—Technology and Engineering. Elsevier, Amsterdam.

Ehlers, S., Elgeti, K., Menzel, T., Wiessmeier, G., 2000. Mixing in the offstream of a microchannel system. Chemical Engineering Process 39, 291–298.

Ehrfeld, W., Golbig, K., Hessel, V., Löwe, H., Richter, T., 1999. Characterization of mixing in micromixers by a test reaction: single mixing units and mixer arrays. Industrial & Engineering Chemistry Research 38, 1075–1082.

Ge, H., Chen, G.W., Yuan, Q., Li, H.Q., 2005. Gas phase catalytic partial oxidation of toluene in a microchannel reactor. Catalysis Today 110, 171–178.

Gerven, T.V., Stankiewicz, A., 2009. Structure, energy, synergy, times—the fundamentals of process intensification. Industrial & Engineering Chemistry Research 48, 2465–2474.

Harmsen, G.J., 2007. Reactive distillation: the front-runner of industrial process intensification—a full review of commercial applications, research, scale-up, design and operation. Chemical Engineering and Processing 46, 774–780.

Hessel, V., Löwe, H., 2003. Microchemical engineering: components, plant concepts user acceptance—Part I. Chemical Engineering & Technology 26, 13–24.

Jähnisch, K., Hessel, V., Löwe, H., Baerns, M., 2004. Chemistry in microstructured reactors. Angewandte Chemie International Edition 43, 406–446.

Khan, S.A., Jensen, K.F., 2007. Microfluidic synthesis of titania shells on colloidal silica. Advanced Material 19, 2556–2560.

Kim, B.J., Yoon, S.Y., Lee, K.H., Sung, H.J., 2009. Development of a microfluidic device for simultaneous mixing and pumping. Experimental Fluids 46, 85–95.

Kochmann, N., 2007. Transport Phenomena in Micro Process Engineering. Springer, New York.

Kronig, R., Brink, H.C., 1950. On the theory of extraction from falling drop. Applied Science Research A 2, 142–156.

Laddha, G.S., Degaleesan, T.E., 1978. Transport Phenomena in Liquid Extraction. McGraw-Hill, New Delhi.

Link, D.R., Anna, S.L., Weitz, D.A., Stone, H.A., 2004. Geometrically mediated breakup of drops in microfluidic devices. Physical Review Letters 92, 054503.

Losey, M.W., Schmidt, M.A., Jensen, K.F., 2001. Microfabricated multiphase packed-bed reactors: characterization of mass transfer and reactions. Industrial & Engineering Chemistry Research 40, 2555–2562.

Matsuyama, K., Tanthapanichakoon, W., Aoki, N., Mae, K., 2007. Operation of microfluidic liquid slug formation and slug design for kinetics measurement. Chemical Engineering Science 62, 5133–5136.

Maruyama, T., Matsushita, H., Uchida, J., Kubota, F., Kamiya, N., Goto, M., 2004a. Liquid membrane operations in a microfluidic device for selective separation of metal ions. Analytical Chemistry 76, 4495–4500.

Maruyama, T., Kaji, T., Ohkawa, T., Sotowa, K., Matsushita, H., Kubota, F., Kamiya, N., Kusakabe, K., Goto, M., 2004b. Intermittent partition walls promote solvent extraction of metal ions in a microfluidic device. Analyst 129, 1008–1013.

Merchuk, J.C., Shai, R., Wolf, D., 1980. Experimental study of copper extraction with LIX-64N by means of motionless mixers. Industrial & Engineering Chemistry Process Design and Development 19, 91–97.

Nagasawa, H., Aoki, N., Mae, K., 2005. Design of a new micromixer for instant mixing based on the collision of micro segments. Chemical Engineering & Technology 28, 324–330.

Odedra, A., Geyer, K., Gustafsson, T., Gilmour, R., Seeberger, P.H., 2008. Safe, facile radical-based reduction and hydrosilylation reactions in a microreactor using tris(trimethylsilyl)silane. Chemical Communication 2008, 3025–3027.

Rowe, P.N., Calxton, R.T., Lewis, T.B., 1965. Heat and mass transfer from a single sphere in an extensive flowing fluid. Transactions of the Institution of Chemical Engineers and the Chemical Engineer 43, 14–31.

SalimiMoosavi, H., Tang, T., Harrison, D.J., 1997. Electroosmotic pumping of organic solvents and reagents in microfabricated reactor chips. Journal of the American Chemical Society 119, 8716–8717.

Schönfeld, F., Hessel, V., Hofmann, C., 2004. An optimised split-and-recombine micro-mixer with uniform 'chaotic' mixing. Lab on a Chip 4, 65–69.

Song, H., Tice, J.D., Ismagilov, R.F., 2003. A microfluidic system for controlling reaction networks in time. Angewandte Chemie International Edition 42, 768–772.

Su, Y.H., Chen, G.W., Zhao, Y.C., Yuan, Q., 2009. Intensification of liquid–liquid two-phase mass transfer by gas agitation in a microchannel. AIChE Journal 55, 1948–1958.

Tice, J.D., Song, H., Lyon, A.D., Ismagilov, R.F., 2003. Formation of droplets and mixing in multiphase microfluidics at low values of the Reynolds and the capillary numbers. Langmuir 19, 9127–9133.

Tokeshi, M., Minagawa, T., Uchiyama, K., Hibara, A., Sato, K., Hisamoto, H., Kitamori, T., 2002. Continuous-flow chemical processing on a microchip by combining microunit operations and a multiphase flow network. Analytical Chemistry 74, 1565–1571.

Utada, A.S., Fernandez, N.A., Gordillo, J.M., Weitz, D.A., 2008. Absolute instability of a liquid jet in a coflowing stream. Physical Review Letters 1, 014502.

Utada, A.S., Lorenceau, E., Link, D.R., Kaplan, P.D., Stone, H.A., Weitz, D.A., 2005. Monodisperse double emulsions generated from a microcapillary device. Science 308, 537–541.

Wiles, C., Watts, P., 2008. Continuous flow reactors, a tool for the modern synthetic chemist. European Journal of Organic Chemistry, 1655–1671.

Ying, Y., Chen, G.W., Zhao, Y.C., Li, S.L., Yuan, Q., 2008. A high throughput methodology for continuous preparation of monodispersed nanocrystals in microfluidic reactors. Chemical Engineering Journal 135, 209–215.

Yue, J., Chen, G.W., Yuan, Q., Luo, L.G., Gonthier, Y., 2007. Hydrodynamics and mass transfer characteristics in gas–liquid flow through a rectangular microchannel. Chemical Engineering Science 62, 2096–2108.

Zhao, Y.C., Chen, G.W., Yuan, Q., 2006. Liquid–liquid two-phase flow patterns in a rectangular microchannel. AIChE Journal 52, 4052–4060.

Zhao, Y.C., Chen, G.W., Yuan, Q., 2007. Liquid–liquid two-phase mass transfer in the T-junction microchannels. AIChE Journal 53, 3042–3053.

Zheng, B., Tice, J.D., Roach, L.S., Ismagilov, R.F., 2004. A droplet-based, composite PDMS/glass capillary microfluidic system for evaluating protein crystallization conditions by microbatch and vapor-diffusion methods with on-chip X-ray diffraction. Angewandte Chemie International Edition 43, 2508–2511.